Residual Flux Measurement of Single-phase Transformers based on Equivalent Resistance

Qingkun Wang[1,2], Yuzhan Ren[1,2], Youhua Wang[1,2], Chengcheng Liu[1,2], and Shipu Wu[1,2]

[1]State Key Laboratory of Reliability and Intelligence of Electrical Equipment
Hebei University of Technology, Tianjin, 300130, China
wqk1501179683@163.com, 1094500481@qq.com

[2]Key Laboratory of Electromagnetic Field and Electrical Apparatus Reliability of Hebei Province
Hebei University of Technology, Tianjin, 300130, China
wangyi@hebut.edu.cn, 2016020@hebut.edu.cn, 601762376@qq.com

Abstract **–** Due to the presence of transformer residual flux, the magnetic flux of the core rapidly reaches saturation, thus causing an inrush current when the no-load transformer is directly connected to the grid, which affects the safe operation of the grid. Therefore, it is necessary to study the residual flux in the core to reduce the inrush current. However, the residual flux estimation has a large error. In this paper, a method is proposed to measure the residual flux of the transformer core by solving equivalent resistance and determining the direction of residual flux by the difference between the forward and reverse transient currents. In addition, the relationship between residual flux and equivalent resistance is established, and the empirical formula is obtained for calculating the residual flux. To evaluate the effectiveness of the proposed method, the residual flux of the square core is measured on the constructed experimental platform. Compared with the experimental results, the relative error of the residual flux of the core calculated by the proposed method is within 6%, which has higher accuracy and provides a reference for residual flux estimation.

Index Terms **–** Equivalent resistance, field-coupled equivalent circuit, residual flux measurement, transformer.

I. INTRODUCTION

The power transformer is an important part of the modern power system, and the working condition of the transformer is directly related to the operation quality of the power grid. The silicon steel sheet used in the transformer core is a ferromagnetic material, and its unique hysteresis generates residual flux, which will not disappear easily once it is generated. When the transformer is closed at no load, it is easy to cause magnetic saturation inside the core under the joint action of steady-state periodic component, transient bias, and residual flux. The generated inrush current transient values can reach up to several times the no-load current, which can cause transformer winding deformation or current imbalance; or it can lead to incorrect operation of relay protection devices and loss of protection of the transformer [1, 2]. In addition, due to the presence of residual flux, the voltage waveform will be distorted and second harmonics will be generated on the grid, affecting the power quality in the power system and causing great damage to the power electronics in the power system [3]. In engineering practice, residual flux measurement has been a pressing problem. The residual flux is difficult to measure directly in the closed core, so most measurement methods in recent years used the relationship between the residual flux and measurable parameters to indirectly obtain information about the residual flux. Faraday's law of electromagnetic induction calculates the residual flux in the transformer core by port voltage integration of power off, which requires a known value of the port voltage of power off [4, 5]. The fluxgate sensor is used to calculate the residual flux value based on the leakage flux, and the measurement results are easily affected by the measurement accuracy of the sensor itself and the installation location [6]. Similarly, the first peak value of the inrush current is used to explore the residual flux change of the transformer, which makes it difficult to directly determine the magnitude of the residual flux [7]. Meanwhile, the minor hysteresis loop is used to determine the residual flux of the transformer. Since the area enclosed by the minor hysteresis loop is indicated as the residual energy, it is unable to represent the direction of the residual flux. Then the charge (a variable) needs to be introduced to determine the direction of the residual flux, which will lead to more calculation errors [8]. In addition, there are two measurement methods, one of which

is calculated by the relationship between the residual flux and current-related parameters [9–11], and the other is an iterative calculation of the dynamic hysteresis model, which has a more complex calculation process [12]. The use of magnetizing inductance to calculate the residual flux in the transformer core is likely to produce large computational errors due to the many external factors affecting the magnetizing inductance, which makes the fitting of the empirical formula difficult [13].

Considering the deficiencies of the existing measurement methods, a method is proposed to calculate the residual flux of the core by solving equivalent resistance and determining the direction of residual flux by the difference between forward and reverse transient currents. Specifically, a small DC signal excitation is applied to measure the current in the transient process. Meanwhile, the equivalent resistance is calculated in the field-coupled equivalent circuit through the measured transient current. Moreover, the relationship between residual flux and equivalent resistance is established. The empirical formulas of each are then used to calculate the residual flux from the equivalent resistance. Finally, the experimental test platform is built to verify the feasibility of the proposed method. The experimental results show that the proposed method has higher accuracy and provides a reference for residual flux estimation.

II. PRINCIPLE OF RESIDUAL FLUX MEASUREMENT

A. Principle of residual flux generation

Most of the ferromagnetic materials used in power transformers are silicon steel sheets, which consist of numerous magnetic domain structures. They can be spontaneously magnetized in microscopic domains, forming tiny magnetic dipoles. The motion of magnetic domains and domain walls has a significant effect on the hysteresis lines and magnetization curves. The magnetization process is divided into domain wall motion and domain rotation motion, shown in Fig. 1. During the magnetization process, if there is no external magnetic field (point O) in Fig. 2, the internal arrangement of magnetic domains is disordered and the magnetic material does not exhibit magnetic properties externally. The magnetic domain starts to move with domain wall displacement and domain rotation in the direction of the applied external magnetic field when the magnetic field is applied. The magnetic domains occur in reversible domain wall displacement motion when the applied magnetic field is small (O-a). If the magnetic field is removed, the domains will return to the starting magnetization state without hysteresis. When the magnetic field is further enhanced, the magnetization process will reach the next state (a-b), and the domain wall motion turns into an irreversible process, accompanied

by a little rotational magnetization. If the magnetic field is removed at this time, the domain wall has reached a new position, the material is still partially magnetized and the magnetic domains are not returned to their initial state. This discontinuous and irregular motion is accompanied by the generation of maximum permeability due to the displacement of the domain walls jumping from one position to another. Meanwhile, noise is generated, which is called "Barkhausen noise." The saturation stage is reached when the applied magnetic field (b-c) increases continuously, the domain wall motion disappears, and the domains are aligned in the same direction as the applied magnetic field. When the magnetization intensity decreases to zero (point d), the magnetic domains and domain walls exhibit the residual flux density because they are unable to fully recover the state before they were magnetized. The hysteresis phenomenon of ferromagnetic materials leads to the residual flux in the core of the power transformer [14].
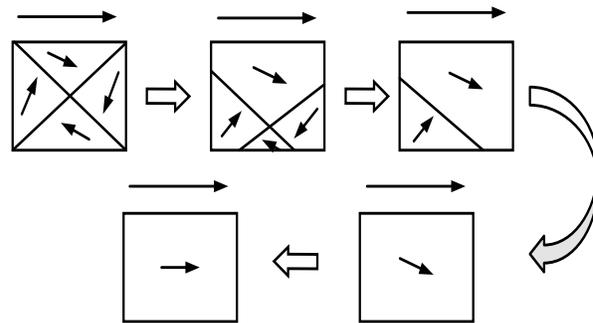
Fig. 1. Structural changes of magnetic domains during magnetization of ferromagnetic materials.
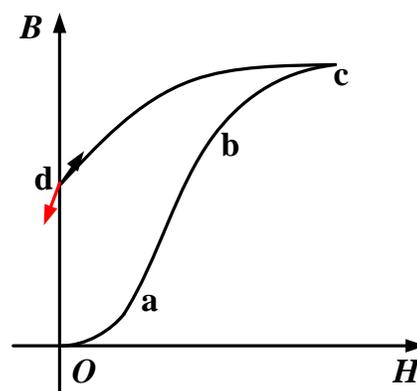
Fig. 2. Hysteresis curve of magnetic material in the transformer core.

B. Forward and reverse current obtainment

Current is obtained by applying a DC voltage of equal amplitude and opposite direction to the transformer

winding. When DC excitation is applied to the core, the leakage flux of the transformer is about 0.15% of the flux during no-load operation, as the permeability of the core silicon steel material is much larger than the air gap permeability. Therefore, the influence of the leakage flux is negligible due to the largest proportion of the main flux. According to the field-coupled equivalent circuit of Fig. 3, the difficult and hard-to-measure magnetic field problem is transformed into a circuit problem [15]. In Fig. 2, the external excitation promotes the magnetization of the core when the DC voltage excitation in the direction of the black arrow is applied. The core is demagnetized when the DC voltage excitation in the direction of the red arrow is applied. Figure 4 shows the significant difference between the forward and reverse currents due to the hysteresis characteristics of the ferromagnetic material. In this case, the current indicated by the faster-changing solid line is the forward excitation current, and the slower-changing dashed line is the reverse excitation current. Therefore, the direction of the residual flux density can be determined by the transient process before reaching the steady state.
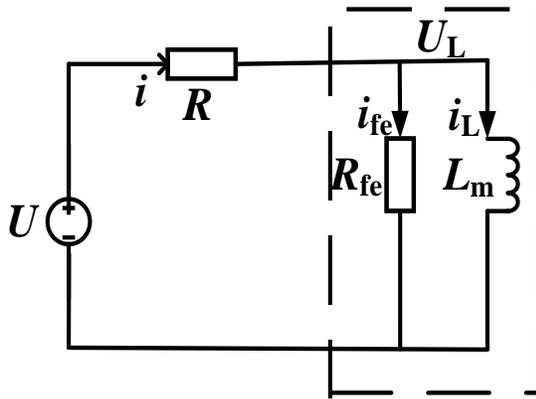
Fig. 3. The equivalent circuit inside the core in the transient process.
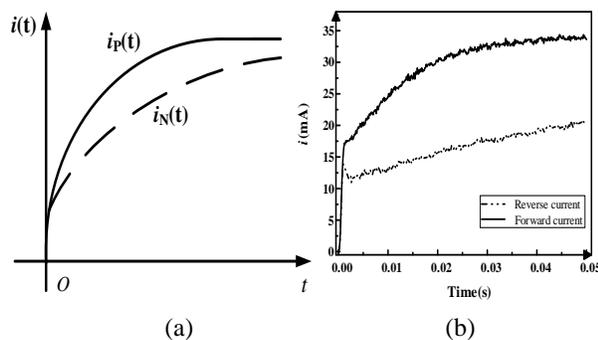
Fig. 4. Transient current diagram: (a) forward and reverse transient current, (b) forward and reverse currents of residual flux at -624 mT.

C. Equivalent resistance calculation

The measured transient currents are post-processed to obtain the relationship between the residual flux density and the equivalent resistance in the field-coupled equivalent circuit. The core is internally equivalent to the resistance and magnetized inductance, and the magnetization process is reflected using the relative differential permeability, which is defined as μ_{rd}, where

$$\mu_{\mathrm{rd}} = \frac{1}{\mu_0}\frac{dB}{dH}. \tag{1}$$

In the process of establishing the magnetic field, the magnetizing inductance of the transformer is calculated by the equation

$$L_{\mathrm{m}} = \frac{N^2 S \mu_0 \mu_{\mathrm{rd}}}{l_{\mathrm{m}}}, \tag{2}$$

where N is the number of turns of the transformer winding, S is the cross-sectional area of the core, l_m is the effective magnetic circuit length, μ_0 is the air permeability, and μ_{rd} is the relative differential permeability of the core material. The Kirchhoff equation is written for the circuit shown in Fig. 3:

$$U = Ri + L_{\mathrm{m}}\frac{di_{\mathrm{L}}}{dt}, \tag{3}$$

$$U_L = L_{\mathrm{m}}\frac{di_{\mathrm{L}}}{dt}, \tag{4}$$

$$i(t) = \left(\frac{U}{R+R_{\mathrm{fe}}} - \frac{U}{R}\right)e^{-\frac{RR_{\mathrm{fe}}}{L_{\mathrm{m}}(R+R_{\mathrm{fe}})}t} + \frac{U}{R}, \tag{5}$$

where R is the series external resistance and R_{fe} is the equivalent resistance of the field-coupled circuit, L_m, is the magnetizing inductance, i_{fe}, is the current flowing through the equivalent resistance, i_L, is the current flowing through the magnetized inductance, I, is the current in the external circuit, U_L is the voltage across the magnetized inductance, and U is the applied DC signal voltage excitation.

As the magnetic flux in the core changes, the equivalent resistance in the core exhibits different characteristics, since the equivalent circuit resistance parameters are determined based on the characteristic parameters of the port current. When a DC voltage excitation is applied to the winding, the transient process value varies with the current [16]. After applying different directions of DC voltage excitation, in the same direction as the residual flux, excitation promotes the magnetization of the core, and reverse excitation demagnetizes. the core. The difference in the equivalent resistance between both is significant.

The change of the forward current is significantly faster than the change of the reverse current after applying DC voltage excitation, due to the difference in the equivalent resistance. Eventually, both reach a steady state, as shown in Fig. 4 (a), and Fig. 4 (b) shows the forward and reverse currents when the residual flux in the transformer core is -624 mT during the experiment.
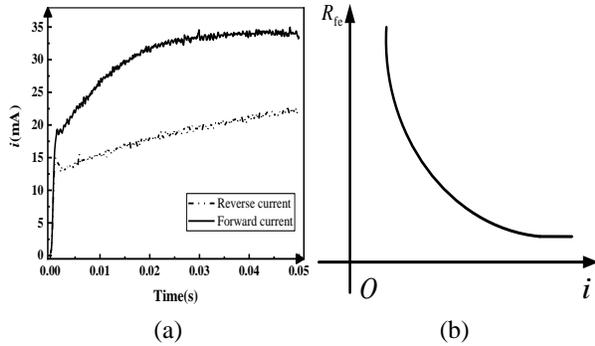
Fig. 5. (a) Forward and reverse currents of residual flux at 791mT, (b) variation curve of equivalent resistance with measured current.

Due to the nonlinear variation of the equivalent resistance, the transient current is varied with different cases of the core flux, and both interact with each other in Fig. 5 (a). Figure 5 (b) shows that as the current increases, the equivalent resistance decreases and eventually tends to a stable value, so there is an obvious inflection point in the variation of the equivalent resistance. Then, to facilitate the determination of the direction of the residual flux density, a forward and reverse voltage excitation is applied to the transformer winding. Under the same residual flux, the applied forward voltage acts as a magnetizing effect on the residual flux of the core, while the applied reverse voltage acts as a demagnetizing effect. Immediately after employing the equivalent resistance calculated by the forward current, the relationship between the equivalent resistance and the residual flux density can be built, and the empirical equation for both can be fitted.

III. SIMULATION CALCULATION ANALYSIS

A. Parameter analysis

The selection of the appropriate DC voltage excitation and energizing time is particularly important. The measurement process is based on the principle of facilitating the measurement of transient processes and not causing changes in the residual flux density in the core. It is ensured that the applied excitation is within the permissible limits for the core for different residual flux cases.

According to Ampere's circuital theorem, the field intensity corresponding to the positive current in the measurement process is H_1 and the negative current is H_2. When the applied voltage excitation produces a field intensity less than H_1 or H_2, the transient current change is not obvious, and it is not possible to determine the direction of residual flux. Hence, the minimum value of H should be greater than the maximum value of both,

and $H_{min} > \max(H_1, H_2)$. Thus the minimum voltage applied is

$$U_{\min} = \frac{H_{\min}Rl}{N}, \qquad (6)$$

where R is the series resistance, l is the average magnetic circuit length, and N is the number of turns of the measurement winding. Moreover, measured flux with no more than 10% of the minimum residual flux is used as a reference to determine the maximum value of applied DC excitation,

$$U_{\max} = \frac{0.1H_c Rl}{N}. \qquad (7)$$

In summary, the selection range of voltage excitation is

$$\frac{H_{\min}Rl}{N} < U < \frac{0.1H_c Rl}{N}, \qquad (8)$$

where H_c is the coercive force of the material.

In the finite element calculation, it is found that the transient current has reached the steady state when the energizing time reaches 50 ms, while too much time will demagnetize the negative residual flux in the transformer core. Finally, the measurement process was designed with an energization time of 50 ms and a DC voltage excitation of 0.15 V.
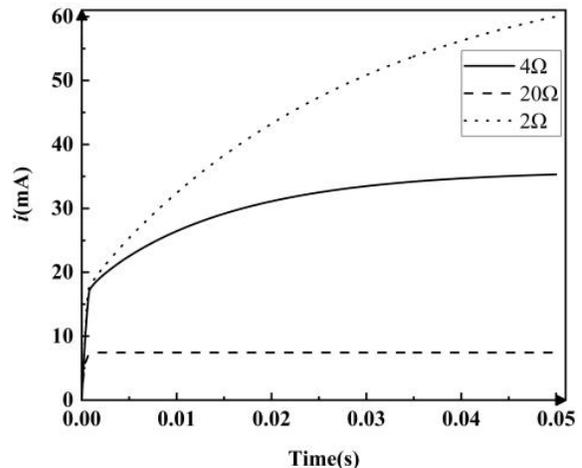
Fig. 6. Transient current under different series resistance.

In the measurement circuits, the magnitude of the current and the time to reach the steady state is more heavily affected by the external series resistance [17]. Therefore, it is necessary to select a suitable series resistance to meet the measurement requirements. Figure 6 shows that when the series resistance is 20 Ω, the value of the current to reach the steady state is small and changes rapidly, which is not conducive to recording the transient process. When the series resistance is 2 Ω, the current has not reached the steady state in 50 ms. Since the series resistor can also play a role in protecting the circuit, the resistance value cannot be chosen too small.

Table 1: Core and circuit parameters

Circuit and Core Parameters	Value
Core material	B30P105
Average magnetic circuit length of the core	1.92 m
Cross-sectional area of the iron core	0.0016 m^2
Density of silicon steel sheets	7.65×10^3 kg/m^3
Square core quality	24 kg
Core saturation magnetic density	1.8 T
Circuit external resistance	4 Ω
Measurement of winding turns	50
Measurement time	50 ms

Fig. 8. Finite element calculation model for the square iron core.

Fig. 7. Schematic diagram of the measurement circuit.

When the 4 Ω resistance is connected in series, the transient process is obvious to record, and the circuit will not be burned due to the small resistance. Finally, for the convenience of analysis and calculation, a series resistance of 4 Ω was chosen.

Based on the design criteria for transformer cores, square cores are used to study transformer cores. The transient characteristics of the equivalent resistance of the transformer core for different residual flux cases are studied. The square core is B30P105 cold-rolled oriented silicon steel sheet, and the model parameters are shown in Table 1. The theoretical saturation magnetic density of the selected B30P105 material is 1.8 T, and the residual flux is generally 0.36 T $\sim$ 1.26 T. According to the measurement theory shown in Fig. 7, the finite element (FEM) calculations in Fig. 8 are performed after selecting the appropriate relevant parameters [18], and the material parameters used in the FEM calculations are derived from the measurements of the constructed experimental platform.

It is essential to establish the relationship between B_r and core material properties to accurately simulate the core under different B_r in finite element calculations. By analyzing the magnetization process in the presence of B_r in the core, the flux density B and the magnetic field intensity H are processed linearly, and the relationship between B and H can be described by the following equation:

$$B(H) = \begin{cases} 0.86 \times 10^{-3}H, & 0 < H \leq 0.45 \\ kH - (k - 0.86 \times 10^{-3})H, & H > 0.45 \end{cases}, \quad (9)$$

where k is related to the residual flux density.

B. The relationship between residual flux and equivalent resistance

For different cases of residual flux in the transformer core, a connection exists between the current and the equivalent resistance, as shown in Fig. 9.
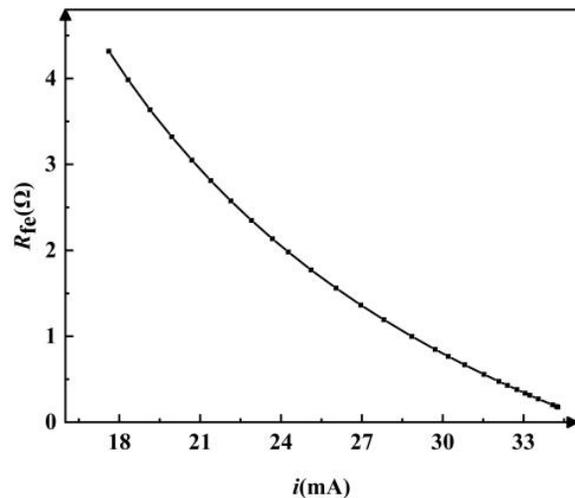
Fig. 9. Variation of equivalent resistance with the current.

The forward and reverse DC voltage excitation of 0.15 V is applied to the primary winding successively, and the direction of the residual flux can be determined by showing that the rate of change of the positive current is greater than that of the negative current, as shown in Fig. 10 (a). The forward current at different residual flux densities is selected, as shown in Fig. 10 (b), and the difference in transient currents exists due to different residual fluxes. The corresponding equivalent resistance is calculated from the forward current to facilitate further calculations of the residual flux, as shown in Fig. 11.

(a)   (b)
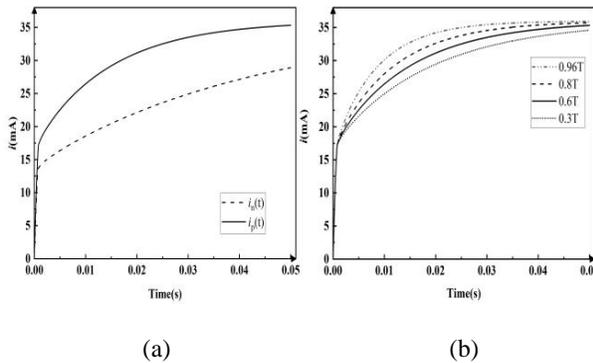
Fig. 10. Calculation of current: (a) comparison of forward and reverse currents at a residual flux density of 0.6 T, (b) comparison of currents under different residual fluxes.
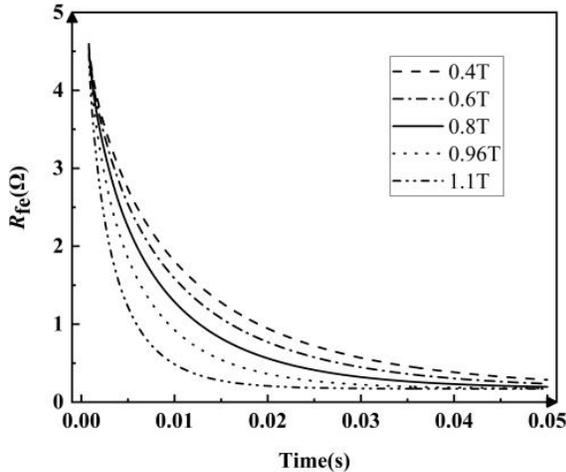
Fig. 11. Variation of equivalent resistance at different residual fluxes.

The direction of the residual flux can be obtained from the analysis of the forward and reverse currents; further, quantitative analysis of the residual flux value can be realized through the equivalent resistance. The equivalent resistance value varies significantly with the

change in residual flux (see Fig. 11). Moreover, the polynomial interpolation method was chosen to fit the curve to the calculated discrete points at the inflection point of the equivalent resistance curve. Figure 12 shows that the discrete points were fitted better by three polynomial interpolations, with a residual sum of squares of 0.00075 and an adjusted R-squared of 0.99848, The empirical formula is fitted by

$$B_\text{r} = -0.309R_\text{fe}{}^3 + 0.494R_\text{fe}{}^2 - 0.839R_\text{fe} + 1.319. \quad (10)$$
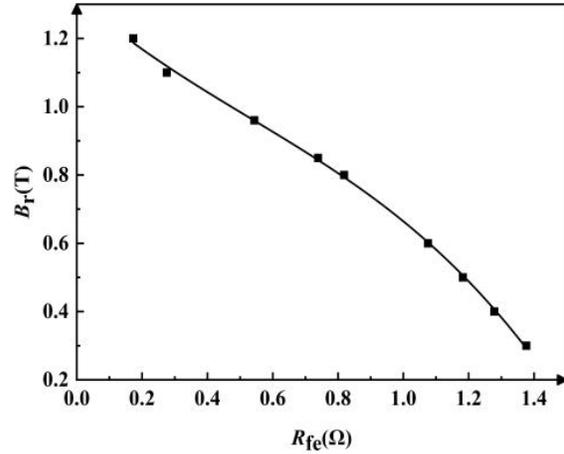
Fig. 12. Empirical formula curve fitting for discrete points.

IV. EXPERIMENTAL MEASUREMENTS AND ANALYSIS OF RESULTS

A. Residual flux preset

To simulate the case of unknown residual flux in engineering, the residual flux of the square core needs to be preset to facilitate comparison with the calculated residual flux. In addition, the core needs to be demagnetized before presetting the residual flux, considering the influence of external conditions to which the core is exposed. During the presetting process, the core is charged with different proportions of saturation flux as a residual flux by DC magnetization, and the applied DC voltage excitation is withdrawn. When the flux density in the core does not change with time, the stable value is recorded as the preset residual flux at this time.

An experimental measurement was performed to verify the feasibility and accuracy of the proposed method by using the experimental measurement platform, as shown in Fig. 13. A signal generator (WF1974) was used to generate the required DC voltage excitation during the experiments and was transmitted to the primary winding of the square core through a power amplifier, and data acquisition was performed using a current probe (N2782B). An oscilloscope (DSOX6004A) was
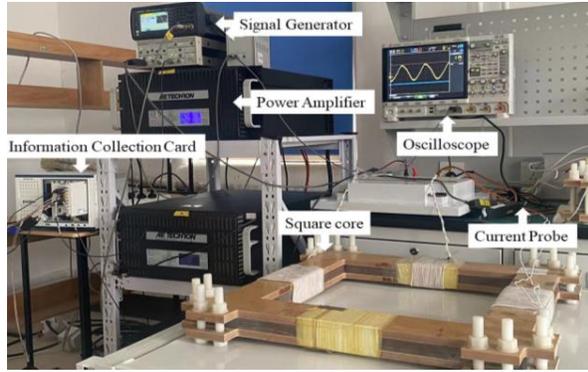
Fig. 13. Experimental measuring devices and square core.

used to record the transient current data, and a flux meter (Flux-meter480) was connected to the secondary winding during the experiments to facilitate the recording of the residual flux variation of the core.

B. Measurement results and analysis

The residual flux of the square core is measured by the experimental platform. The measurement system and the transmission system generate random errors and random noise, so noise effects are inevitable during the experiments. The measured transient currents are filtered using the moving average filter method. Figure 14 (a) compares the current finite element calculations of the residual flux of the core with the experimentally measured current values. It can be seen that the calculated values are similar to the experimentally measured values, so the calculated equivalent resistance values in Fig. 14 (b) are more accurate.
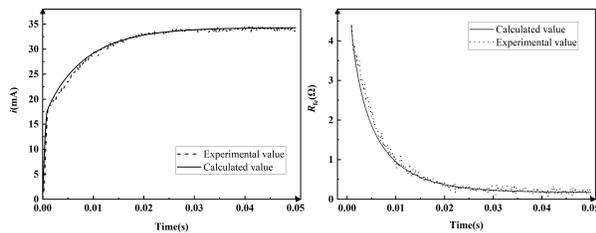
Fig. 14. Comparison of experimental measurements and calculations: (a) calculated and experimental transient current, (b) calculated with an experimental equivalent resistance.

The fitted empirical formula is employed for the residual flux calculation and compared with the presetting value. The error rate is defined as

$$\varepsilon = \left| \frac{B_{rc} - B_r}{B_r} \right| \times 100\%, \qquad (11)$$

where B_{rc} is the calculated residual flux value, and B_r is the experimental preset residual flux value. Therefore,

Table 2: Relative error between experimental and calculated values

B_r(mT)	$R_{fe}(\Omega)$	B_{rc}(mT)	$\varepsilon(\%)$
489	1.22	467.89	4.32
624	1.08	598.61	4.07
714	0.98	679.44	4.84
791	0.89	745.01	5.81
915	0.57	943.78	3.10
954	0.51	978.41	2.56

the reliability of the measurement method is checked by the error rate.

Table 2 shows the residual flux value and the error based on the calculated and experimental values. The maximum error occurred at 791 mT and the error rate of 5.81%, while the minimum error of 2.56% occurred at 954 mT. Considering the influence of many factors such as measurement equipment, surrounding external environment, and data post-processing, the measurement error is less than 10%, which can meet the requirement.

V. CONCLUSION

This paper is based on the electromagnetic transient process of the core magnetic material after applying DC voltage excitation, by measuring the forward and reverse currents for different residual flux density cases. The forward current is selected as the target, and the corresponding equivalent resistance is calculated in the field-coupled equivalent circuit. Then, the relationship between the equivalent resistance and the residual flux is established, and the empirical equation for calculation is obtained. Finally, the method is verified by establishing an experimental test platform, and if the measurement results show that the relative error of the measured residual flux in the core is within 6%, the residual flux in the transformer core can be measured accurately. The advantage of the method is that it does not require the known state of the transformer before the power outage and has high measurement accuracy while meeting practical engineering requirements. Therefore, the method provides a reference for the estimation of residual flux.

REFERENCES

[1] C. Chuanjiang, F. Chun-en, X. Yang, L. Wei, Z. Bi-de, and R. Xiao, "Experimental study on controlled unloaded transformer switching considering residual flux"' *2017 4th International Conference on Electric Power Equipment - Switching Technology (ICEPE-ST)*, Xi'an, China, 2017.

[2] W. S. Fonseca, D. S. Lima, A. K. F. Lima, M. V. A. Nunes, U. H. Bezerra, and N. S. Soeiro, "Analysis of Structural Behavior of Transformer's Winding

Under Inrush Current Conditions," *IEEE Transactions on Industry Applications*, vol. 54, no. 3, pp. 2285-2294, May-June 2018.

[3] E. Cardelli, A. Faba, and F. Tissi, "Prediction and Control of Transformer Inrush Currents," *IEEE Transactions on Magnetics*, vol. 51, no. 3, pp. 1-4, March 2015.

[4] W. Yuan, H. Zhang, Y. Shangguan, J. Zou, and J. Yuan, "Analysis on method of calculating transformer residual flux by using the integration of port-voltage waveform and its implementation," *2017 20th International Conference on Electrical Machines and Systems (ICEMS)*, Sydney, NSW, Australia, 2017.

[5] K. Wang, G. Li, and S. Zhang, "Research on residual flux characteristics of transformer with single-phase four-limb core under different dc excitation current," *2020 IEEE International Conference on High Voltage Engineering and Application (ICHVE)*, Beijing, China, 2020.

[6] D. Cavallera, V. Oiring, J.-L. Coulomb, O. Chadebec, B. Caillault, and F. Zgainski, "A new method to evaluate residual flux thanks to leakage flux, application to a transformer," *IEEE Transactions on Magnetics*, vol. 50, no. 2, pp. 1005-1008, Feb. 2014.

[7] T. Peng, D. Wan, M. Zhao, H. Zhou, L. Mao, and X. Duan, "An indirect method for measuring transformer residual magnetism," *2019 IEEE 3rd Conference on Energy Internet and Energy System Integration (EI2)*, Changsha, China, pp. 1084-1087, 2019.

[8] D. Vulin, K. Milicevic, I. Biondic, and G. Petrovic, "Determining the residual magnetic flux value of a single-phase transformer using a minor hysteresis loop," *IEEE Transactions on Power Delivery*, vol. 36, no. 4, pp. 2066-2074, Aug. 2021.

[9] C. Huo, Y. Wang, S. Wu, and C. Liu, "Research on residual flux density measurement for single-phase transformer core based on energy changes," *IEEE Transactions on Instrumentation and Measurement*, vol. 70, pp. 1-9, 2021.

[10] W. Ge, Y. Wang, Z. Zhao, X. Yang, and Y. Li, "Residual flux in the closed magnetic core of a power transformer," *IEEE Transactions on Applied Superconductivity*, vol. 24, no. 3, pp. 1-4, June 2014.

[11] S. Wu, Y. Ren, Y. Wang, C. Huo, and C. Liu, "Residual flux measurement of power transformer based on transient current difference," *IEEE Transactions on Magnetics*, vol. 58, no. 2, pp. 1-5, Feb. 2022.

[12] Y. Wang, Z. Liu, and H. Chen, "Research on residual flux prediction of the transformer," *IEEE Transactions on Magnetics*, vol. 53, no. 6, pp. 1-4, June 2017.

[13] C. Huo, Y. Wang, C. Liu, and G. Lei, "Study on the residual flux density measurement method for power transformer cores based on magnetising inductance," *IET Electric Power Applications*, vol. 16, no. 2, pp. 224-235, 2022.

[14] M. Ouili, R. Mehasni, M. Feliachi, H. Allag, H. Bouchekara, G. Berthiau, and M. Latreche, "Coupling of 3D analytical calculation and PSO for the identification of magnet parameters used in magnetic separation," *Applied Computational Electromagnetics Society (ACES) Journal,* pp. 1607-1615, 2019.

[15] E. Gomez, A. Gabaldón, A. Molina, and J. Roger-Folch, "Coupling 2D finite element models and circuit equations using a bottom-up methodology," *The Applied Computational Electromagnetics Society (ACES) Journal,* pp. 225-231, 2002.

[16] M. Jafarifar, B. Rezaeealam, and A. Mir, "A new approach for improving the load current characteristic of cascaded magnetic flux compression generator," *Applied Computational Electromagnetics Society (ACES) Journal,* vol. 34, no. 8, pp. 1134-1142, 2019.

[17] F. G. Montoya, F. D. León, F. Arrabal-Campos, and A. Alcayde, "determination of instantaneous powers from a novel time-domain parameter identification method of non-linear single-phase circuits," *IEEE Transactions on Power Delivery*, vol. 37, no. 5, pp. 3608-3619, Oct. 2022.

[18] J. Ge, H. H. Eldeeb, K. Liu, J. Kang, H. Zhao, and O. Mohammed,, "Optimal range of coupling coefficient of loosely coupled transformer considering system resistance," *Applied Computational Electromagnetics Society (ACES) Journal*, vol. 35, no. 11, pp. 1368-1369, Nov. 2020.

Qingkun Wang was born in Jining, Shandong, China, in 1998. He received a B.E. degree in electrical engineering from Binzhou University, Binzhou, China, in 2021. He is currently pursuing an M.E. degree in electrical engineering at the Hebei University of Technology, Tianjin, China. His current research interest is the measurement of the residual flux of the power transformer core.

Yuzhan Ren was born in Anhui, China, in 1997. He received a B.E. degree in electrical engineering from Northeast Electric Power University, Jilin, China, in 2019. He is currently pursuing a Ph.D. degree in electrical engineering from the Hebei University of Technology, Tianjin, China. His current research interests include measurement of the residual flux of power transformer cores and research on the inrush current of large power transformers.

Youhua Wang was born in Jiujiang, Jiangxi, China, in 1964. He received a B.E. degree from Xian Jiaotong University, Xian, China, in 1987, an M.E. degree from the Hebei University of Technology, Tianjin, China, in 1990, and a Ph.D. from Fuzhou University, Fuzhou, China, in 1994, all in electrical apparatus. He is currently a professor at the College of Electrical Engineering. His current research interests include measurement and modeling of properties of magnetic materials, numerical analysis of the electromagnetic field, and electromagnetic device design, analysis, and optimization.

Chengcheng Liu was born in Jiangsu, China, in 1988. He received a B.E. degree in automation engineering from Yangzhou University, Yangzhou, China, in 2010, and a Ph.D. degree in electrical engineering from the Hebei University of Technology, Tianjin, China, in 2016. He was a joint Ph.D. student supported by the Chinese scholarship council with the University of Technology, Sydney, NSW, Australia. He is currently an IEEE member and an associate professor at the Hebei University of Technology. His research interests include the design, analysis, control, and optimization of electromagnetic devices.

Shipu Wu was born in Shijiazhuang, Hebei, China, in 1995. He received a B.E. degree in electrical engineering from the Hebei University of Technology, Tianjin, China, in 2017. He is currently pursuing a Ph.D. degree in electrical engineering at the Hebei University of Technology, Tianjin, China. His current research interests include measurement of the residual flux of power transformer cores and research on the inrush current of large power transformers.